universe

IMPACT FACTOR 2.9

CITESCORE 3.6

Article

New Localization Method of Abelian Gauge Fields on Bloch Branes

Yi Zhong and Yun-Zhi Du

MDPI

https://doi.org/10.3390/universe9100450

universe

MDPI

Article

New Localization Method of Abelian Gauge Fields on Bloch Branes

Yi Zhong [1,2] and Yun-Zhi Du [3,4,*]

[1] School of Physics and Electronics Science, Hunan University, Changsha 410082, China; zhongy@hnu.edu.cn
[2] Lanzhou Center for Theoretical Physics, Key Laboratory of Theoretical Physics of Gansu Province, School of Physical Science and Technology, Lanzhou University, Lanzhou 730000, China
[3] Department of Physics, Shanxi Datong University, Datong 037009, China
[4] Institute of Theoretical Physics, Shanxi Datong University, Datong 037009, China
* Correspondence: duyzh22@sxdtdx.edu.cn

Abstract: In this paper, we study the localization of the five-dimensional $U(1)$ gauge field coupled with a background scalar potential on symmetric and asymmetric degenerate Bloch branes. By decomposing the $U(1)$ gauge field A_M into its vector part ($\hat{A}_M$) and scalar components, we found that the Lagrangian of the five-dimensional $U(1)$ gauge field can be rewritten as two independent parts: one for the vector field and the other for two scalar fields. Regarding the vector part, the effective potential exhibits a volcano-like shape with finite depth. We obtain a massless vector field on both types of Bloch branes and a set of massive KK resonances. For the scalar part, their massless modes are coupled with each other, while two sets of massive scalar KK modes are independent. Similar to the vector effective potential, the scalar potentials create infinite wells for both types of degenerate Bloch brane solutions. Therefore, there is only one independent massless scalar mode and two sets of massive scalar Kaluza–Klein resonances. Furthermore, we also observed that, for the two types of Bloch brane solutions, the asymmetric parameter c_0 has different effects on the localization of scalar modes.

Keywords: brane world; localization; gauge field

Citation: Zhong, Y.; Du, Y.-Z. New Localization Method of Abelian Gauge Fields on Bloch Branes. *Universe* **2023**, *9*, 450. https://doi.org/10.3390/universe9100450

Academic Editor: Biagio Lucini

Received: 5 September 2023
Revised: 11 October 2023
Accepted: 13 October 2023
Published: 16 October 2023

1. Introduction

In the past two decades, extra dimension theory has been a widely studied and researched field. Among others, the Randall–Sundrum (RS) model [1,2] and ADD model [3,4] have attracted widespread attention. A primary motivation behind these brane world models is to tackle the hierarchy problem, which involves addressing the 16 orders of magnitude disparity between the Planck scale and the electroweak scale. In the context of brane world theory, the bulk space is often described as a five-dimensional AdS (anti-de Sitter) spacetime, establishing a potential connection with the AdS/QCD framework. Consequently, this study may enhance our understanding of the intricate interplay between extra dimensions and their potential implications in the realm of strong interactions and hadron physics. In the RS models and ADD model, the branes are infinitely thin, which could lead to a singularity on the brane. Therefore, the thick brane generated by a background was proposed [5–8] and further generalized into the Bloch brane model with an internal structure, generated by two interacting scalar fields [9]. In the Bloch brane model, it was found that the variation of a parameter associated to the domain wall degeneracy can control the thickness of the brane. This specific model is called the degenerate Bloch brane [10]. The acceleration of the universe was investigated in the degenerate Bloch brane [11].

An essential condition for these brane world models is to provide an explanation for why our observed world, at the energy scales currently explored, seems to possess only three spatial dimensions. The answer, which has been given in these brane world models,

is that all particles/fields in the standard model should be localized on a $3+1$ dimensional brane in higher dimensional spacetime. Hence, we need localization mechanisms for various matter fields to make our universe appear effectively $3+1$ dimensional up to some energy scale. Free scalar fields can usually be localized to branes [12,13]. On the other hand, fermion fields typically necessitate Yukawa couplings with background scalar fields to achieve localization on branes [14,15]. Nevertheless, the localization of vector fields on a flat brane in five dimensions is generally considered to be challenging. Attempts have been made to solve the problem of localizing the vector field on a brane, with the main methods including the following: assuming that the vector field interacts with the background scalar field [16], considering models such as the Weyl geometry brane world [17], and assuming that the vector field has a nonminimal coupling with spacetime metric [18]. In Ref. [19], it was found that the vector field can be localized by adding a dynamical mass term into the standard five-dimensional action of the vector field, which is proportional to the five-dimensional scalar curvature. It was shown that the vector zero mode is localizable if the five-dimensional spacetime is (asymptotic) anti-de Sitter. Moreover, the massive tachyonic modes can be excluded [19].

On the other hand, the Stueckelberg action was proposed to restore the gauge symmetry of the massive gauge field by introducing an auxiliary scalar field [20]. Recently, inspired by the Stueckelberg mechanism, the localization of the vector field is facilitated by the incorporation of Stueckelberg-compensating fields into the 5D action of a gauge field. In this setup, the quadratic coefficient of the gauge fields is designed to mimic a Yukawa-like brane–gauge coupling [21]. It was found that the zero mode of the gauge field can be localized on the brane through the establishment of an appropriate coupling function between the brane and the gauge field, and this mechanism is also studied for the localization of the Kalb–Ramond field [21]. Moreover, localization of abelian gauge fields with Stueckelberg-like geometrical coupling on an $f(T,B)$-thick brane was also investigated, and it was found that the Stueckelberg-like geometrical coupling can localize the massless mode of the transverse component of the gauge vector and the Kalb–Ramond fields.

Furthermore, it was found that, due to the internal structure of the Bloch branes and degenerate Bloch branes, the localization of matter fields exhibits new features [22–26]. Therefore, we will investigate the localization of a Stüeckelberg-like vector field on the symmetric and asymmetric degenerate Bloch branes.

The layout of the paper is as follows: In Section 2, we briefly provide a review of the Bloch brane model. In Section 3, we explore the localization of an abelian gauge field on the symmetric and asymmetric degenerate Bloch branes. Finally, we conclude with a discussion of our findings in Section 4.

2. Review of Bloch Brane Model

In this work, we consider the thick branes generated by two real scalar fields, ϕ and ξ, with a potential $V(\phi,\xi)$, which describes the interacting between the two scalar fields. The action for such a system is given by

$$S=\int d^5x\,\sqrt{-g}\left[\frac{1}{4}R-\frac{1}{2}(\partial^M\phi\partial_M\phi+\partial^M\xi\partial_M\xi)-V(\phi,\xi)\right], \tag{1}$$

where g is the determinant of the metric tensor g_{MN}, R stands for the scalar curvature of the bulk, and the capital letters M and N range from 0 to 4. The two scalar fields ϕ and ξ depend solely on the physical coordinate y in the case of a static flat brane. It is an interesting model that gives rise to an internal structure in the energy density of the brane, depending on the specific choice of the potential $V(\phi,\xi)$.

The line element describing a flat brane is assumed to be

$$ds^2=e^{2A}\eta_{\mu\nu}dx^\mu dx^\nu+dy^2, \tag{2}$$

where e^{2A} represents the warp factor, and the four-dimensional Minkowski metric $\eta_{\mu\nu} = diag(-1,1,1,1)$. With this metric, we can obtain the equation of motion:

$$\phi'' + 4A'\phi' - \frac{\partial V(\phi,\xi)}{\partial\phi} = 0, \tag{3}$$

$$\xi'' + 4A'\xi' - \frac{\partial V(\phi,\xi)}{\partial\xi} = 0, \tag{4}$$

$$A'^2 - \frac{1}{6}\left(\phi'^2 + \xi'^2\right) + \frac{1}{3}V(\phi,\xi) = 0, \tag{5}$$

$$A'' + \frac{2}{3}\left(\phi'^2 + \xi'^2\right) = 0, \tag{6}$$

where the prime denotes the derivative with respect to the extra dimension coordinate y. Solving the above equations analytically is not easy, since there exists the couplings between the functions involved in the model and some of them are of second order. In Refs. [27–29], the authors introduced a superpotential $W(\phi,\xi)$ and implement a first-order formalism; thus, one can obtain the following first-order differential equations:

$$\phi' = \frac{\partial W(\phi,\xi)}{\partial\phi}, \quad \xi' = \frac{\partial W(\phi,\xi)}{\partial\xi}, \quad A' = -\frac{2}{3}W(\phi,\xi), \tag{7}$$

and the potential of the background scalar fields is determined in terms of $W(\phi,\xi)$ by

$$V = \frac{1}{2}\left[\left(\frac{\partial W(\phi,\xi)}{\partial\phi}\right)^2 + \left(\frac{\partial W(\phi,\xi)}{\partial\xi}\right)^2\right] - \frac{4}{3}W^2(\phi,\xi). \tag{8}$$

In this work, we consider degenerate Bloch branes. We will briefly review two type of degenerate Bloch brane solutions, and the detailed derivation can be found in Ref. [28]. We assume a superpotential of the following form with four parameters: v, a, b, and β [10,28]

$$W(\phi,\xi) = \phi\left[a\left(v^2 - \frac{1}{3}\phi^2\right) - b\xi^2\right] + \frac{3}{2}\beta \tag{9}$$

The corresponding solutions represent two kinds of asymmetric degenerate Bloch branes for the $a = b$ and $a = 4b$, respectively. And the parameter β is related to the asymmetry of the branes.

2.1. Case I: Degenerate I Bloch Brane

To obtain the degenerate I Bloch brane solution, we assume $c_0 < -2$ and $a = b$. The asymmetric degenerate Bloch brane solutions are solved as follows [10,28]:

$$\phi(y) = \frac{\sqrt{c_0^2-4}\, v \sinh(2bvy)}{\sqrt{c_0^2-4}\cosh(2bvy) - c_0}, \tag{10a}$$

$$\xi(y) = \frac{2v}{\sqrt{c_0^2-4}\cosh(2bvy) - c_0}, \tag{10b}$$

$$\begin{aligned} A(y) = {} & \frac{2v^2\left(-\sqrt{c_0^2-4}\, c_0 \cosh(2bvy) + c_0^2 - 4\right)}{9\left(\sqrt{c_0^2-4}\cosh(2bvy) - c_0\right)^2} - \frac{2v^2(c_0^2 - \sqrt{c_0^2-4}\, c_0 - 4)}{9(\sqrt{c_0^2-4} - c_0)^2} \\ & + \log\left(\frac{\sqrt{c_0^2-4} - c_0}{\sqrt{c_0^2-4}\cosh(2bvy) - c_0}\right)^{\frac{2v^2}{9}} - \beta y \end{aligned} \tag{10c}$$

2.2. Case II: Degenerate II Bloch Brane

To obtain the degenerate II Bloch brane solution, we assume $c_0 < 1/16$ and $a = 4b$. The asymmetric degenerate Bloch brane solutions are solved as follows [10,28]:

$$\phi(y) = \frac{\sqrt{1-16c_0}\, v \sinh(4bvy)}{1+\sqrt{1-16c_0}\cosh(4bvy)}, \tag{11a}$$

$$\xi(y) = \frac{2v}{\sqrt{1+\sqrt{1-16c_0}\cosh(4bvy)}}, \tag{11b}$$

$$e^{2A(y)} = \left\{\frac{1+\sqrt{1-16c_0}}{1+\sqrt{1-16c_0}\cosh(4bvy)}\right\}^{\frac{8v^2}{9}} \times \exp\left[\frac{4v^2(1+8c_0+\sqrt{1-16c_0})}{9(1+\sqrt{1-16c_0})^2}\right] \times \exp\left\{-\frac{4v^2\left[1+8c_0+\sqrt{1-16c_0}\cosh(4bvy)\right]}{9\left[1+\sqrt{1-16c_0}\cosh(4bvy)\right]^2} - 2\beta y\right\} \tag{11c}$$

Note that for both two cases, β is the asymmetric parameter, as $\beta \to 0$, the above asymmetric solutions reduce to symmetric ones. These solutions reveal that the Bloch brane has a rich internal structure. The details of these solutions can be found in Refs. [9,10]. In addition, since $A(y) - \beta y$ should be a finite value as $y \to \pm\infty$, the parameter β must satisfy the constraint

$$|\beta| \leq \frac{4av^3}{9}. \tag{12}$$

The shapes of the background scalar potential for the symmetric and asymmetric degenerate Bloch branes are plotted in Figures 1 and 2. The thickness of the degenerate branes could be described by the parameter δ as

$$\delta = \begin{cases} \frac{1}{bv}\ln\frac{-2c_0}{u_1} & \text{for the degenerate I Bloch brane solution (10) as } c_0 \to -2 \\ \frac{1}{2bv}\ln\frac{6}{u_2} & \text{for the degenerate II Bloch brane solution (11) as } c_0 \to \frac{1}{16} \end{cases}, \tag{13}$$

where we defined the constants u_1 and u_2 as follows for convenience:

$$u_1 \equiv \sqrt{c_0^2-4}, \qquad u_2 \equiv \sqrt{1-16c_0}. \tag{14}$$

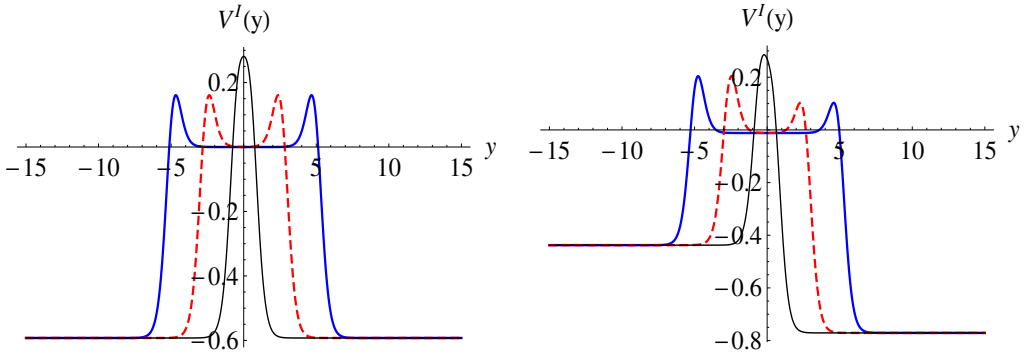

Figure 1. The shapes of the background scalar potential $V(y)$ for the symmetric ($\beta = 0$, (**left**)) and asymmetric ($\beta = 1/16$, (**right**)) degenerate I Bloch branes with $a = b$. The parameters are set to $b = 1$, $v = 1$, $c_0 = -2 - 10^{-8}$ for the thick blue lines, $c_0 = -2 - 10^{-4}$ for the dashed red lines, and $c_0 = -2.5$ for the thin black lines.

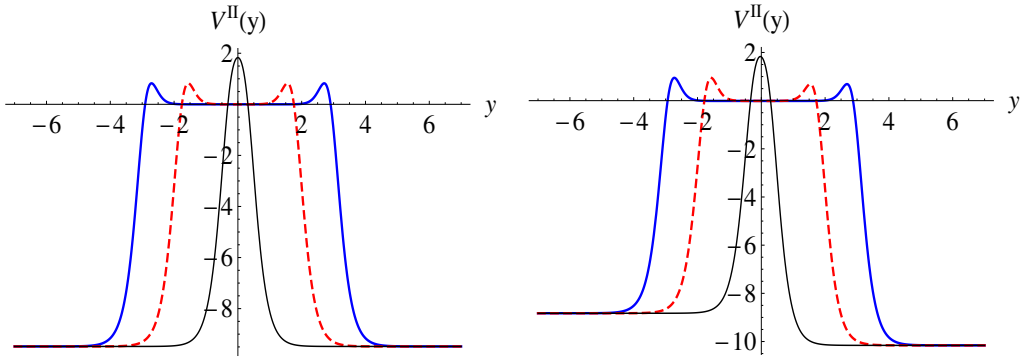

Figure 2. The shapes of the background scalar potential $V(y)$ for the symmetric ($\beta = 0$, (**left**)) and asymmetric ($\beta = 1/16$, (**right**)) degenerate II Bloch branes with $a = 4b$. The parameters are set to $b = 1$, $v = 1$, $c_0 = \frac{1}{16+10^{-8}}$ for the thick blue lines, $c_0 = \frac{1}{16+10^{-4}}$ for the dashed red lines, and $c_0 = 0.01$ for the thin black lines.

Note that the single brane is localized at $y = 0$, while the two sub-branes are localized at $y = \pm\frac{\delta}{2}$ and the thickness of the double brane is δ. In the following, we mainly discuss the degenerate Bloch solutions in the case of double branes. The degenerate I double Bloch brane corresponds to $u_1 \to 0$, and the degenerate II double Bloch brane corresponds to $u_2 \to 0$. Furthermore, the thickness of degenerate double Bloch branes is independent of the asymmetric parameter β.

In this work, we focus on the localization of the gauge vector field coupled to the background scalar potential $V(\phi, \xi)$ in both asymmetric and symmetric degenerate Bloch solutions, referred to as degenerate I and degenerate II Bloch brane solutions, respectively.

3. Localization of Abelian Gauge Field

Inspired by the paper [21], we explore the Stüeckelberg-like vector field action with the coupling to the background potential in the five-dimensional spacetime as follows:

$$S = \int d^5 x \sqrt{-g} \left[-\frac{1}{4} F^{MN} F_{MN} - \eta V(\phi, \xi)(\partial_M B - A_M)^2 \right], \tag{15}$$

where η is a coupling constant, and $V(\phi, \xi)$ is the background scalar potential. A_M is the five-dimensional gauge vector field and B is the Stüeckelberg scalar field. This action exhibits gauge symmetry under the following transformations:

$$A_M \to A_M + \partial_M \Lambda, \quad B \to B + \Lambda. \tag{16}$$

In this part, we mainly investigate the existence of the zero mode and the massive Kaluza–Klein (KK) modes of U(1) vector field on degenerated Bloch branes by choosing the particular coupling parameter η.

3.1. Equation of Motion and Decoupling Actions

The equations of motion for the fields A_M, B can be obtained by varying the action (15) with respect to the corresponding fields:

$$\partial_M [\sqrt{-g}\, F^{MN}] = -2\eta \sqrt{-g}\, V(\phi, \xi)(\partial^N B - A^N), \tag{17}$$

$$\partial_M \left[\sqrt{-g}\, V(\phi, \xi)(\partial^M B - A^M) \right] = 0, \tag{18}$$

where Equation (18) is consistent with the Noether's identity obtained by taking the divergence of Equation (17).

In the following, our analysis was used to fix the gauge. Instead of imposing an explicit gauge fixing condition, we performed an analogous analysis as in Ref. [30], where the five-dimensional field A_M is parameterized as

$$A_M = (A_\mu, A_4) = (\hat{A}_\mu + \partial_\mu \psi, A_4) \tag{19}$$

with $\hat{A}_\mu$ and ψ as the transverse ($\partial^\mu \hat{A}_\mu = 0$) and longitudinal components of A_μ, respectively. Under gauge transformation (16), these components behavior are

$$\hat{A}_\mu \to \hat{A}_\mu, \;\; A_4 \to A_4 + \lambda', \;\; \psi \to \psi + \lambda, \;\; B \to B + \lambda. \tag{20}$$

We can redefine the scalar degrees of freedom as follows:

$$\lambda = A_4 - \psi', \;\; \rho = B - \psi, \tag{21}$$

which remain invariant under the gauge transformation (20). The parameterization defined by Equations (19) and (21) is equivalent to choosing the gauge condition $\partial_\mu A^\mu = 0$.

Then, considering the parameterized fields $\hat{A}_\mu$, λ, ρ, Equations (17) and (18) can be rewritten as

$$\left\{\Box + e^{2A}\left[\partial_y^2 + 2A'\partial_y - 2\eta V(\phi,\xi)\right]\right\}\hat{A}_\nu = 0, \tag{22}$$

$$\partial_y(e^{2A}\lambda) - 2e^{2A}\eta V(\phi,\xi)\rho = 0, \tag{23}$$

$$e^{2A}\Box\lambda + 2e^{4A}\eta V(\phi,\xi)(\rho' - \lambda) = 0, \tag{24}$$

$$2e^{2A}\eta V(\phi,\xi)\Box\rho + \partial_y\left[2e^{4A}\eta V(\phi,\xi)\right] = 0. \tag{25}$$

Moreover, we can reformulate the action, as denoted in (15), using invariant components. It can be demonstrated that the transverse vector $\hat{A}_\mu$ becomes decoupled from the scalar fields as follows:

$$S_A = S_{\hat{A}} + S_S, \tag{26}$$

$$S_{\hat{A}} = \int d^5x \left[-\frac{1}{4}\hat{F}_{\mu\nu}^2 - \frac{1}{2}e^{2A}(\hat{A}'_\mu)^2 - \eta V(\phi,\xi)e^{2A}\hat{A}_\mu^2\right], \tag{27}$$

$$S_S = \int d^5x \left[-\frac{1}{2}(\partial_\mu\lambda)^2 - e^{2A}\eta V(\phi,\xi)(\partial_\mu\rho)^2 - e^{4A}\eta V(\phi,\xi)(\lambda - \rho')^2\right]. \tag{28}$$

It is evident that the equation for the vector degree, as shown in Equation (22), can be readily derived from $S_{\hat{A}}$. Similarly, the equations for the scalar degrees, as expressed in Equations (24) and (25), originate from S_S.

3.2. Localization of Vector Degree $\hat{A}^\mu$

Next, we examine the localization for the vector degree $\hat{A}_\mu$ by taking into account the coupling with the background scalar potential $\eta V(\phi,\xi)$. The gauge field is decomposed as follows:

$$\hat{A}_\mu = \sum_n a_\mu^{(n)}(x)\alpha_n(y), \tag{29}$$

and then the equation of motion for the vector degree (22) reduces to

$$\left[\partial_y^2 + 2A'\partial_y - 2\eta V(\phi,\xi)\right]\alpha_n(y) = -e^{-2A}m_n^2\alpha_n(y) \tag{30}$$

with $\Box a_\mu^{(n)}(x) = m_n^2 a_\mu^{(n)}(x)$.

Then, we work in the conformal coordinate x^μ, z, and redefine $\alpha_n(y) = e^{-\frac{A}{2}}\bar{\alpha}_n(z)$ and substitute the background scalar potential (5) into Equation (30). As a result, the equation governing the vector degree modes transforms into a Schrödinger-like equation:

$$\left[-\partial_z^2 + U_A(z)\right]\bar{\alpha}_n(z) = m_n^2\bar{\alpha}_n(z), \tag{31}$$

in which the effective potential $U_A(z)$ is given by

$$U_A(z) = \left(\frac{1}{2} - \frac{3}{2}\eta\right)\ddot{A} + \left(\frac{1}{4} - \frac{9}{2}\eta\right)\dot{A}^2. \tag{32}$$

Here, the dot denotes derivative with respect to z. Usually, the Schrödinger Equation (31) is difficult to solve analytically. A common method for solving equations of this type is the factorize method, which demands that Equation (31) can be factorized, and we can factorize Equation (31) as

$$Q^\dagger Q\bar{\alpha}_n(z) = m_n^2\bar{\alpha}_n(z), \tag{33}$$

where $Q = -\partial_z + p\dot{A}$, and p is a constant that is related to the parameter η. After simple calculations, we can obtain

$$Q^\dagger Q = -\partial_z^2 + \left(p^2\dot{A}^2 + p\ddot{A}\right). \tag{34}$$

Comparing the above equation with Equations (31) and (32), we can obtain the condition under which Equation (31) can be factorized, i.e., $p = \frac{5}{2}$ and $\eta = -\frac{4}{3}$. And the hermiticity and positive definiteness of $Q^\dagger Q$ in Equation (33) ensure that no normalizable negative energy modes are allowed. Therefore, we will assume this condition in the following since otherwise the Schrödinger Equation (31) is difficult to solve analytically and tachyonic modes may exist.

Furthermore, we need to impose the orthonormality condition

$$\int_{-\infty}^{\infty} dy\ \alpha_n(y)\alpha_l(y) = \int_{-\infty}^{\infty} dz\ \bar{\alpha}_n(z)\bar{\alpha}_l(z) = \delta_{nl}, \tag{35}$$

in order to obtain the effective four-dimensional action for the gauge field $a_\mu^{(n)}(x)$:

$$S_{\hat{A}} = \sum_n \int d^4x \left\{-\frac{1}{4}f_{\mu\nu}^{(n)}f_{(n)}^{\mu\nu} - \frac{1}{2}m_n^2 a_\mu^{(n)}a_{(n)}^\mu\right\} \tag{36}$$

with the four-dimensional gauge field strength tensor $f_{\mu\nu}^{(n)} = \partial_\mu a_\nu^{(n)} - \partial_\nu a_\mu^{(n)}$. This action represents an action of a four-dimensional massless gauge field and a series of massive vector fields on the brane. Therefore, we can utilize the orthonormality condition (35) to determine if the Kaluza–Klein modes of the gauge field can be localized on the degenerate Bloch branes.

On the other hand, the massless wave function

$$\bar{\alpha}_0(z) = k_0 e^{\frac{5}{2}A}, \tag{37}$$

is normalizable, and the corresponding the zero-mode $\alpha_0(y)$ turns out to be

$$\alpha_0(y) = k_0 e^{2A}. \tag{38}$$

Here, k_0 is the normalization constant determined by the orthonormality condition (35).

Given that the function $y(z)$ cannot be explicitly defined for the brane solutions mentioned in the preceding section, we can represent the effective potential $\mathrm{U}_A(z)$ as a function of the physical coordinate:

$$\mathrm{U}_A(z(y)) = e^{2A}\left\{\frac{5}{2}\partial_y^2 A(y) + \frac{35}{4}\left[\partial_y A(y)\right]^2\right\}. \tag{39}$$

Then, we can use the numerical relation between y and z, $y = y(z)$, to obtain $\mathrm{U}_A(z)$ from above equation.

For the asymmetric degenerate Bloch brane solutions, the explicit expressions of $\mathrm{U}_A(z(y))$ read

$$\begin{aligned}
\mathrm{U}_A^{\mathrm{I}}(z(y)) &= \left\{\frac{u_1 - c_0}{u_1\cosh(2vby) - c_0}\right\}^{\frac{4v^2}{9}} \exp^{\frac{4v^2u_1}{9}\left\{\frac{u_1 - c_0\cosh(2vby)}{[c_0 - u_1\cosh(2vby)]^2} - \frac{1}{u_1 - c_0}\right\} - 2\beta y} \frac{5}{324[c_0 - u_1\cosh(2vby)]^6} \\
&\left\{216b^2u_1^2v^4[c_0 - u_1\cosh(2vby)]^2[-3u_1^2 + 4c_0u_1\cosh(2vby) + (-2c_0^2 + u_1^2)\cosh(4vby)]\right. \\
&+7\{-9c_0^3\beta + u_1[27c_0^2\beta\cosh(2vby) - 27c_0u_1\beta\cosh(2vby)^2 + 9u_1^2\beta\cosh(2vby)^3 \\
&\left.+bu_1v^3(9u_1\sinh(2vby) - 6c_0\sinh(4vby) + u_1\sinh(6vby))]\}^2\right\},
\end{aligned} \tag{40}$$

$$\begin{aligned}
\mathrm{U}_A^{\mathrm{II}}(z(y)) &= \left\{\frac{1 + u_2}{1 + u_2\cosh(4bvy)}\right\}^{\frac{8v^2}{9}} \exp^{\frac{4v^2}{9}\left[\frac{1+8c_0+u_2}{(1+u_2)^2} - \frac{1+8c_0+u_2\cosh(4bvy)}{(1+u_2\cosh(4bvy))^2}\right] - 2\beta y} \\
&\times\frac{5}{324}\left\{567\beta^2 + \frac{1008\, bv^3u_2^2\left\{3\cosh(4bvy) + u_2\left[2 + \cosh(8bvy)\right]\right\}\sinh(4bvy)}{[1 + u_2\cosh(4bvy)]^3}\right. \\
&-\frac{16\, b^2u_2^2v^4}{[1 + u_2\cosh(4bvy)]^6}\{27\left[1 + u_2\cosh(4bvy)\right]^2\left[4\left(u_2^2 + \cosh(8bvy)\right) + u_2\left(7\cosh(4bvy)\right.\right. \\
&\left.\left.+\cosh(12bvy)\right)\right] - 28v^2[3u_2\cosh(4bvy) + u_2^2\left(2 + \cosh(8bvy)\right)]^2\sinh^2(4bvy)\}\Big\}.
\end{aligned} \tag{41}$$

The corresponding zero mode wave functions for the asymmetric degenerate I and II Bloch brane solutions are

$$\bar{\alpha}_0^{\mathrm{I,II}}(z(y)) \propto \bar{\alpha}_0^{\mathrm{IS,IIS}}(z(y))\exp^{-2\beta y}, \tag{42}$$

where $\bar{\alpha}_0^{\mathrm{IS,IIS}}(z(y))$ are the zero mode solutions for the symmetric degenerate Bloch branes case, given by

$$\bar{\alpha}_0^{\mathrm{IS}}(z(y)) = \left\{\frac{u_1 - c_0}{u_1\cosh(2vby) - c_0}\right\}^{\frac{4v^2}{9}} \exp^{\frac{4v^2u_1}{9}\left[\frac{u_1 - c_0\cosh(2vby)}{(c_0 - u_1\cosh(2vby))^2} - \frac{1}{u_1 - c_0}\right]}, \tag{43}$$

$$\bar{\alpha}_0^{\mathrm{IIS}}(z(y)) = \left\{\frac{1 + u_2}{1 + u_2\cosh(4bvy)}\right\}^{\frac{8v^2}{9}} \exp^{\frac{4v^2}{9}\left[\frac{1+8c_0+u_2}{(1+u_2)^2} - \frac{1+8c_0+u_2\cosh(4bvy)}{(1+u_2\cosh(4bvy))^2}\right]}. \tag{44}$$

The zero wave functions $\bar{\alpha}_0^{\mathrm{I,II}}(z(y))$ and effective potentials $\mathrm{U}_A^{\mathrm{I,II}}(z(y))$ of the vector field with different parameters c_0 for two degenerate Bloch brane solutions are plotted in Figures 3 and 4. From these profiles, we can observe that, when $u_i \ll 1$ for both $i = 1$ and $i = 2$, the branes exhibit a dual sub-brane structure. Additionally, the effective potentials $\mathrm{U}_A^{\mathrm{I,II}}$ feature two subwells positioned at $y = \pm\frac{\delta}{2}$ (as shown in Figures 3 and 4). For the degenerate I Bloch brane solution, the zero mode $\bar{\alpha}_0(z(y))$ remains constant between the two sub-branes in the case of symmetric branes, while it becomes localized on the left sub-brane for asymmetric branes. Conversely, in the degenerate II Bloch brane solution, the zero mode $\bar{\alpha}_0(z(y))$ does not remain constant between the two sub-branes, regardless of whether the branes are symmetric or asymmetric. Instead, it becomes localized at the midpoint between the two

sub-branes. The zero mode represents the four-dimensional vector field and serves as the lowest energy eigenfunction (ground state) of the Schrödinger-like Equation (31) due to its absence of zeros.

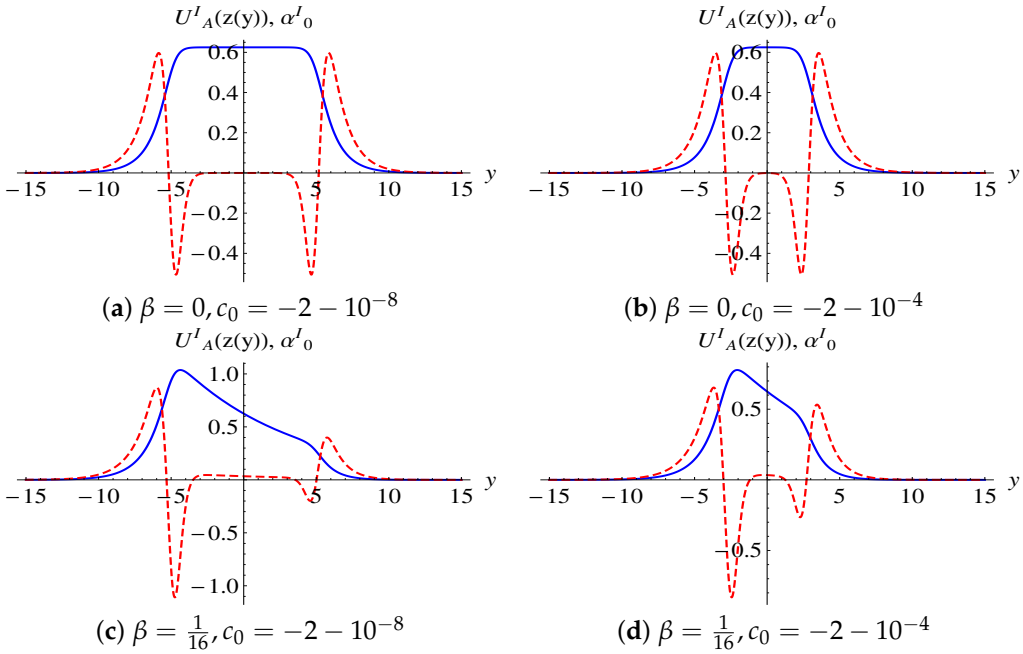

(**a**) $\beta = 0, c_0 = -2 - 10^{-8}$ (**b**) $\beta = 0, c_0 = -2 - 10^{-4}$

(**c**) $\beta = \frac{1}{16}, c_0 = -2 - 10^{-8}$ (**d**) $\beta = \frac{1}{16}, c_0 = -2 - 10^{-4}$

Figure 3. The shapes of the massless profile for vector field $\bar{\alpha}_0^{\mathrm{I}}(z(y))$ (the thickness lines) and the effective potential $\mathrm{U}_A^{\mathrm{I}}(z(y))$ (the dashed lines). The parameters b, v are set to $b = v = 1$.

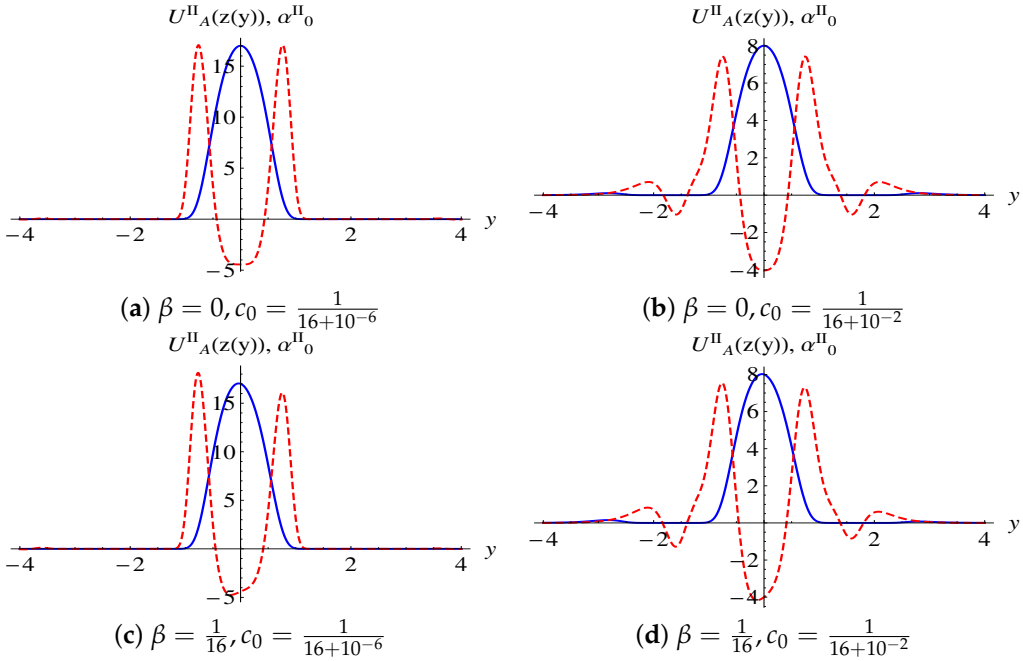

(**a**) $\beta = 0, c_0 = \frac{1}{16+10^{-6}}$ (**b**) $\beta = 0, c_0 = \frac{1}{16+10^{-2}}$

(**c**) $\beta = \frac{1}{16}, c_0 = \frac{1}{16+10^{-6}}$ (**d**) $\beta = \frac{1}{16}, c_0 = \frac{1}{16+10^{-2}}$

Figure 4. The shapes of the massless profile for vector field $\bar{\alpha}_0^{\mathrm{II}}(z(y))$ (the thickness lines) and the effective potential $\mathrm{U}_A^{\mathrm{II}}(z(y))$ (the dashed lines). The parameters b, v are set to $b = v = 1$.

The behavior of $\bar{\alpha}_n^{\mathrm{I,II}}(z(y))$ is governed by the characteristics of the effective potentials $\mathrm{U}_A^{\mathrm{I,II}}$. The values of effective potentials at $y = 0$ and $y \to \pm\infty$ are

$$\mathrm{U}_A^{\mathrm{I}}(z(0)) = -\frac{20b^2u_1^2v^4}{3(c_0-u_1)^2} + \frac{35\beta^2}{4}, \quad \mathrm{U}_A^{\mathrm{I}}(z(y\to\pm\infty)) \to 0, \tag{45}$$

$$\mathrm{U}_A^{\mathrm{II}}(z(0)) = -\frac{80b^2u_2^2v^4}{3(1+u_2)^2} + \frac{35\beta^2}{4}, \quad \mathrm{U}_A^{\mathrm{II}}(z(y\to\pm\infty)) \to 0. \tag{46}$$

Given that $\mathrm{U}_A \to 0$ as $z \to \pm\infty$ for both degenerate Bloch brane solutions, there is no discernible mass gap to distinguish the zero mode from the excited KK modes. In other words, a gapless and continuous spectrum of KK modes exists. The massive modes propagate along the extra dimension, and those with lower energy gradually dissipate due to the presence of potential barriers in the vicinity of the brane locations.

The behavior of the potentials depend on the parameter u_i (or c_0). When $u_i \to 0$, two subwells appear at the locations of the two corresponding sub-branes, which could be related to the resonances. And the resonances may remarkably affect the modifications of the four-dimensional Clumb's law at distances. In what follows, we investigate the massive modes of the vector field by numerically solving Equation (31) with the effective potentials (40) and (41). In Refs. [31,32], the relative probability method was introduced to investigate the resonance of matter fields for the symmetry effective potential. The relative probability function is of m_n, which is defined in a box with borders at $\pm z_{max}$:

$$P(m_n) = \frac{\int_{-z_b}^{z_b} |\bar{\alpha}_n(z)|^2 dz}{\int_{-z_{max}}^{z_{max}} |\bar{\alpha}_n(z)|^2 dz}, \tag{47}$$

where $z_{max} = 10z_b$ and $2z_b$ is about the thickness of the brane.

In this scenario, we are examining the condition where $m_n^2 < \mathrm{U}_{A\ max}^{\mathrm{I,II}}$. The substantial relative probability of massive KK modes within the interval $-z_b < z < z_b$ suggests the presence of resonances. However, due to the symmetry of the potential, the wave functions exhibit either even-parity or odd-parity. Thus, they give two additional initial conditions to obtain the solutions of $\bar{\alpha}_n(z)$ from the Equation (31):

$$\bar{\alpha}_n(0) = 0, \ \bar{\alpha}_n'(0) = 1, \quad \text{for} \quad \text{odd-parity}, \tag{48}$$

$$\bar{\alpha}_n(0) = 1, \ \bar{\alpha}_n'(0) = 0, \quad \text{for} \quad \text{even-parity}. \tag{49}$$

Here, we show the relative probability $P(m_n)$ of massive KK resonances with different parameter v for the symmetric degenerate I and II Bloch branes ($\beta = 0$) in Figures 5 and 6, and the parameters are set to $b = 1$, $c_0 = -2 - 10^{-8}$.

3.3. Localization of Scalar Degree Sector

Now, we analyze the properties of the scalar sector in this model. We start with the decomposition of scalar fields ρ and λ as

$$\rho(x,y) = \sum_n \rho_n(x)\gamma_n(y), \qquad \lambda(x,y) = \sum_n \lambda_n(x)\beta_n(y), \tag{50}$$

where $\Box\rho_n(x) = m_{Sn}^2\rho_n(x)$, $\Box\lambda_n(x) = m_{Sn}^2\lambda_n(x)$. For the massless modes, considering Equations (24) and (25), we have the relation

$$\rho_0(x)\gamma_0'(y) = \lambda_0(x)\beta_0(y). \tag{51}$$

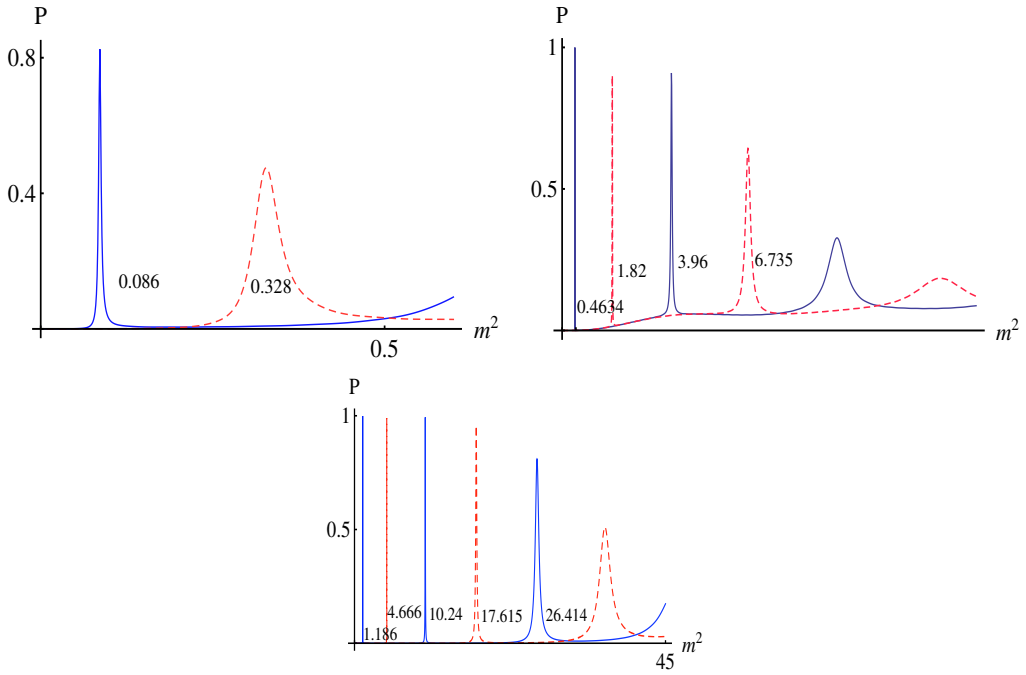

Figure 5. The profiles of the relative probability $P(m_n)$ of vector KK resonances for the symmetric degenerate I Bloch branes ($\beta = 0$). The parameters are set to $b = 1$, $c_0 = -2 - 10^{-8}$. The blue lines stand for the odd modes, and the red dashed lines stand for the even modes.

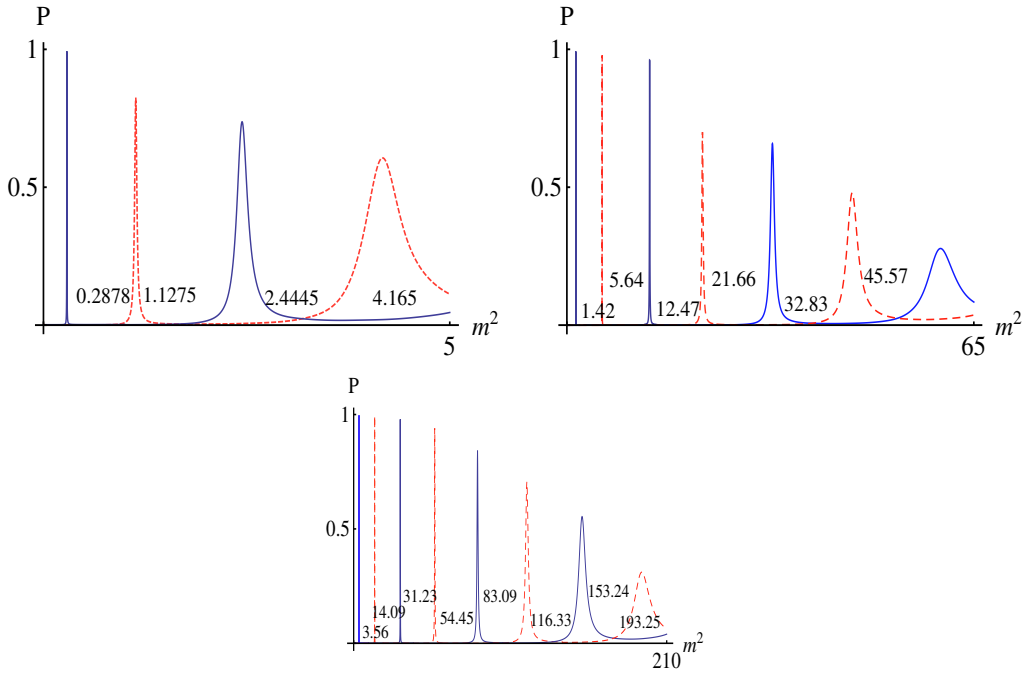

Figure 6. The profiles of the relative probability $P(m_n)$ of vector KK resonances for the symmetric degenerate II Bloch branes ($\beta = 0$). The parameters are set to $b = 1$, $c_0 = \frac{1}{16+10^{-8}}$. The blue lines stand for the odd modes, and the red dashed lines stand for the even modes.

Substituting Equation (51) into (23), we find that the equation of the massless scalar field ρ coincides with Equation (30) in the massless case, i.e.,

$$(\partial_y^2 + 2A'\partial_y - 2\eta V)\gamma_0 = 0. \tag{52}$$

Therefore, as $\eta = -\frac{4}{3}$, the zero mode reads

$$\gamma_0(y) = k_{s0} e^{2A}, \tag{53}$$

which is of same properties as the massless vector mode for degenerate I and II Bloch branes.

Now, we should check whether this massless scalar mode satisfies its orthonormality condition. Therefore, substituting massless scalar modes into the action of scalar degrees (28) and using the relation (51), we have

$$S_{S_0} = \int d^4x \left\{ -\frac{1}{2}\partial_\mu \rho_0 \partial^\mu \rho_0 \right\} \int dy\, e^{2A} \left(\gamma_0'^2 - \frac{8}{3} V \gamma_0^2 \right) \tag{54}$$

with the background scalar potential $V = -3\left(A'^2 + \frac{1}{4}A''\right)$. From the above equation, it seems that there is only one massless scalar mode. Since the integral

$$\int_{-\infty}^{\infty} dy\, e^{2A} \left(\gamma_0'^2 - \frac{8}{3} V \gamma_0^2 \right) = \int_{-\infty}^{\infty} dy\, k_{s0}^2 e^{6A} (12A'^2 + 2A'') \tag{55}$$

is a positive finite value, the conclusion that only one massless scalar mode survives on the degenerate Bloch branes is consistent with that given before. It is very different from the result shown in Ref. [21], where the authors indicated no massless scalar mode on the branes.

In the following, we rely on the equations of motion to analyze massive scalar modes. Substituting the KK decompositions (50) into Equation (23), we can obtain

$$\partial_y (e^{2A} \beta_n) \lambda_n = 2 e^{2A} \eta V(\phi, \xi) \rho_n \gamma_n. \tag{56}$$

From Equation (24), the massive KK modes of two scalar fields satisfy

$$\beta_n \Box \lambda_n + 2 e^{2A} \eta V(\phi, \xi)(\rho_n \gamma_n' - \lambda_n \beta_n) = 0. \tag{57}$$

Combining the above equation and (56), and then canceling the scalar field ρ, we have

$$-\partial_y^2 (e^{2A} \beta_n) + \left(2A' + \frac{V'}{V} \right) \partial_y (e^{2A} \beta_n) + 2\eta V e^{2A} \beta_n = m_{Sn}^2 \beta_n. \tag{58}$$

Note that the parameter η is fixed to $-\frac{4}{3}$. Switching to the conformal coordinate z, $\beta_n(y) = V^{1/2} e^{-\frac{1}{2}A} \bar{\beta}_n(z)$, and plugging the background scalar potential (5) into the above equation, the equation for KK modes of the scalar field λ becomes

$$\left[-\partial_z^2 + U_S(z(y)) \right] \bar{\beta}_n(z) = m_{Sn}^2 \bar{\beta}_n(z) \tag{59}$$

with the effective potential $U_S(z(y))$

$$U_S(z(y)) = \left(\frac{35}{4} A'^2 + \frac{1}{2} A'' + \frac{A'V'}{2V} + \frac{3V'^2}{4V^2} - \frac{V''}{2V} \right) e^{2A}, \tag{60}$$

where the background scalar potential $V = -3\left(A'^2 + \frac{1}{4}A''\right)$.

Since the expressions of effective potential $U_S(z(y))$ are very complex after substituting the asymmetry degenerate Bloch brane solutions into Equation (60), here we only display the profile of $U_S(z(y))$ with different parameters (see Figures 7 and 8). It is clear that the effective potential is an infinite single well such as $\beta = 0$ for the symmetric degenerate I and II Bloch solutions, while for the asymmetric degenerate Bloch solutions $\beta = 1/16$, there are infinite wells when $c_0 - 2 \gg 0$ (asymmetry degenerate I Bloch) or $c_0 - 2 \gg 0$

(asymmetry degenerate II Bloch). Therefore, there is a zero mode and a set of massive KK modes for the scalar λ, which can be obtained by solving Equation (59) numerically. Then, substituting the KK modes β_n into the coupling equations of scalar degrees, we can also obtain the KK modes of the scalar field ρ, which do not hold up in the following.

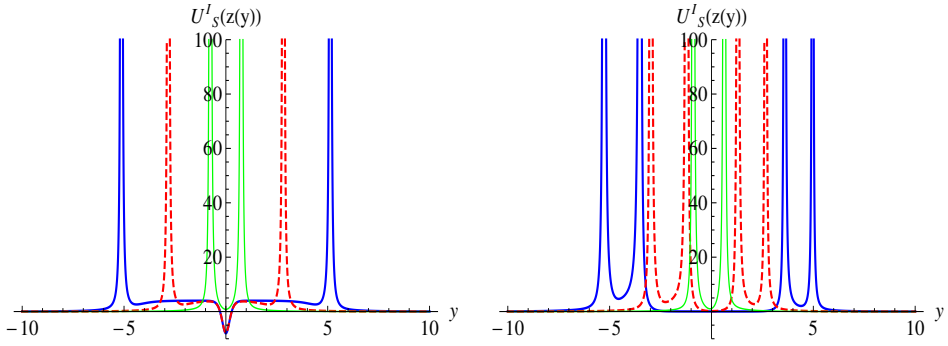

(**a**) $\beta = 0$ (**b**) $\beta = 1/16$

Figure 7. The effective potential $U^{II}_S(z(y))$ for the scalar field λ with different parameters in the degenerate I Bloch brane world. The parameters are set to: $b = v = 1$; $c_0 = -2 - 10^{-8}$ (thick blue lines); $c_0 = -2 - 10^{-4}$ (dashed red lines); $c_0 = -2.5$ (thin green lines).

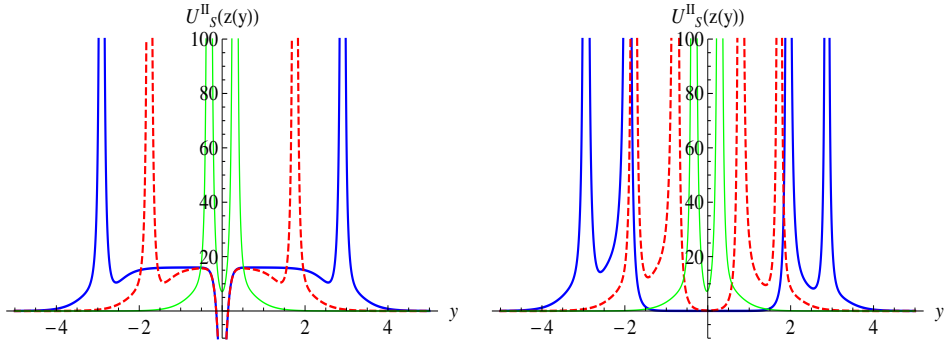

(**a**) $\beta = 0$ (**b**) $\beta = 1/16$

Figure 8. The effective potential $U^{II}_S(z(y))$ of the scalar field λ with different parameters in the degenerate II Bloch brane world. The parameters are set to: $b = v = 1$; $c_0 = \frac{1}{16+10^{-8}}$ (thick blue lines); $c_0 = \frac{1}{16+10^{-4}}$ (dashed red lines); $c_0 = 0.01$ (thin green lines).

4. Conclusions

In this paper, we examine the localization of the $U(1)$ gauge field coupled to the scalar potential on symmetric and asymmetric degenerate Bloch branes. The Bloch brane solutions are characterized by four parameters (b, v, c_0, β), where v influences the thickness of the brane, β solely determines the degree of asymmetry of the brane, and c_0 impacts both the width and depth of the brane. Moreover, for the asymmetric degenerate I (or II) Bloch brane, when $b = v = 1$, $c_0 - 2 \ll 0$, (or $b = v = 1$, $c_0 - 1/16 \ll 0$), these branes are double (or single).

Firstly, we decomposed the five-dimensional $U(1)$ gauge field A_M into one vector degree of freedom and two scalar degrees of freedom, which are independent of each other. For the vector part, we obtained the massless vector field on the two types of Bloch branes and a set of massive KK resonances. As the parameter v increases, more and more massive KK resonances emerge, since the effective potential of the vector KK modes deepens. For the scalar part, there are two types of scalar fields. The massless scalar fields are coupled with each other, while two sets of massive scalar KK modes are independent. Similar to the vector effective potential, both types of scalar effective potentials are infinite wells for the two types of degenerate Bloch brane solutions. Therefore, there is only one massless scalar mode and two sets of independent infinite massive KK resonances.

Next, we explored the effect of the parameter c_0 on the localization of scalar modes. The results indicated that, for the symmetric degenerate I Bloch brane, the effective potential becomes narrower as c_0 decreases. However, for the II Bloch brane, the opposite is true. As c_0 decreases, the effective potential transitions from double wells to a single well for the asymmetric degenerate I Bloch brane. This change also applies to the asymmetric degenerate II brane as c_0 increases. We will consider other coupling methods for the gauge field to obtain the four-dimensional zero mode in future work, such as the coupling with the Einstein tensor $G_{MN}A^MA^N$, with the Ricci tensor $R_{MN}A^MA^N$, or with the energy momentum of matter fields $T_{MN}A^MA^N$.

Author Contributions: Writing, review and editing, Y.Z. and Y.-Z.D. All authors have read and agreed to the published version of the manuscript.

Funding: This research was funded by the Natural Science Foundation of Hunan Province, China (Grant No. 2022JJ40033), and the National Natural Science Foundation of China (Grant No. 12247101).

Data Availability Statement: Our research data is fully disclosed within the paper.

Conflicts of Interest: The authors declare no conflict of interest.

References

1. Randall, L.; Sundrum, R. A large mass hierarchy from a small extra dimension. *Phys. Rev. Lett.* **1999**, *83*, 3370. [CrossRef]
2. Randall, L.; Sundrum, R. An alternative to compactification. *Phys. Rev. Lett.* **1999**, *83*, 4690. [CrossRef]
3. Arkani-Hamed, N.; Dimopoulos, S.; Dvali, G. The hierarchy problem and new dimensions at a millimeter. *Phys. Lett.* **1998**, *29*, 263–272. [CrossRef]
4. Antoniadis, I.; Arkani-Hamed, N.; Dimopoulos, S.; Dvali, G. New dimensions at a millimeter to a fermi and superstrings at a Tev. *Phys. Lett.* **1998**, *436*, 257–263. [CrossRef]
5. Gremm, M. Thick domain walls and singular spaces. *Phys. Rev. D Part. Fields* **2000**, *62*, 044017. [CrossRef]
6. Gass, R.; Mukherjee, M. Domain wall space-times and particle motion. *Phys. Rev.* **1999**, *60*, 065011.
7. Gremm, M. Four-dimensional gravity on a thick domain wall. *Phys. Lett. B* **2000**, *478*, 434–438. [CrossRef]
8. Afonso, V.I.; Bazeia, D.; Losano, L. First-order formalism for bent brane. *Phys. Lett. B* **2006**, *634*, 526–530. [CrossRef]
9. Bazeia, D.; Gomes, A.R. Bloch brane. *J. High Energy Phys.* **2004**, *2004*, 012. [CrossRef]
10. de Souza Dutra, A.; de Faria, A.C.A., Jr.; Hott, M. Degenerate and critical bloch branes. *Phys. Rev. D Part. Fields* **2008**, *78*, 043526. [CrossRef]
11. de Souza Dutra, A.; Amaro de Faria, A.C., Jr.; Hott, M. Degenerate and critical domain walls and accelerating universes driven by bulk particles. *arXiv* **2009**, arXiv:0903.5533.
12. Bajc, B.; Gabadadze, G. Localization of matter and cosmological constant on a brane in anti de sitter space. *Phys. Lett. B* **2000**, *474*, 282–291. [CrossRef]
13. Oda, I. Localization of matters on a string-like defect. *Phys. Lett. B* **2000**, *496*, 113–121. [CrossRef]
14. Melfo, A.; Pantoja, N.; Tempo, J.D. Fermion localization on thick branes. *Phys. Rev. D Part. Fields* **2006**, *73*, 04403. [CrossRef]
15. Liang, J.; Duan, Y.-S. Localization and mass spectrum of spin-1/2 fermionic field on a thick brane with poincare symmetry. *Europhys. Lett.* **2009**, *87*, 40005. [CrossRef]
16. Chumbes, A.E.R.; da Silva, J.M.H.; Hott, M.B. A model to localize gauge and tensor fields on thick branes. *Phys. Rev. D* **2012**, *85*, 085003. [CrossRef]
17. Barbosa-Cendejas, N.; Herrera-Aguilar, A. Localization of 4-d gravity on pure geometrical thick branes. *Phys. Rev. DPart. Fields* **2006**, *73*, 084022. [CrossRef]
18. Alencar, G.; Landim, R.; Tahim, M.; Filho, R.C. Gauge field localization on the brane through geometrical coupling. *Phys. Lett. B* **2014**, *739*, 125–127. [CrossRef]
19. Zhao, Z.-H.; Xie, Q.-Y.; Zhong, Y. New localization method of u(1) gauge vector field on flat branes in (asymptotic) ads_5 spacetime. *Class. Quantum Gravity* **2015**, *32*, 035020. [CrossRef]
20. Stueckelberg, E.C.G. Interaction energy in electrodynamics and in the field theory of nuclear forces. *Helv. Phys. Acta* **1938**, *11*, 225–244.
21. Vaquera-Araujo, C.A.; Corradini, O. Localization of abelian gauge fields on thick branes. *Eur. Phys. J. C Part. Fields* **2015**, *75*, 48. [CrossRef]
22. Belchior, F.M.; Moreira, A.R.P.; Maluf, R.V.; Almeida, C.A.S. Localization of abelian gauge fields with stueckelberg-like geometrical coupling on f(t, b)-thick brane. *Eur. Phys. J. C Part. Fields* **2023**, *83*, 388. [CrossRef]
23. Correa, R.A.C.; de Souza Dutra, A.; Hott, M.B. Fermion localization on degenerate and critical branes. *Class. Quantum Grav.* **2011**, *28*, 155012. [CrossRef]
24. Cruz, W.T.; Lima, A.R.P.; Almeida, C.A.S. Gauge field localization on the bloch brane. *Phys. Rev. D Part. Fields* **2013**, *87*, 045018. [CrossRef]

25. Xie, Q.-Y.; Zhao, Z.-H.; Yang, J.; Yang, K. Fermion localization and degenerate resonances on brane array. *Class. Quantum Gravity* **2019**, *37*, 025012. [CrossRef]
26. Zhao, Z.-H.; Liu, Y.-X.; Zhong, Y. U(1) gauge field localization on a bloch brane with chumbes-holf da silva-hott mechanism. *Phys. Rev. D Part. Fields* **2014**, *90*, 045031. [CrossRef]
27. Bazeia, D.; Ferreira, D.A.; Marques, M.A. Internal structure of cuscuton Bloch brane. *Eur. Phys. J. C* **2021**, *81*, 619. [CrossRef]
28. Xie, Q.-Y.; Yang, J.; Zhao, L. Resonance mass spectra of gravity and fermion on bloch branes. *Phys. Rev. D Part. Fields* **2013**, *88*, 105014. [CrossRef]
29. Guerrero, R.; Melfo, A.; Pantoja, N.; Rodriguez, R.O. Close to the edge: Hierarchy in a double braneworld. *Phys. Rev. D Part. Fields* **2006**, *74*, 084025. [CrossRef]
30. Batell, B.; Gherghetta, T. Yang-mills localization in warped space. *Phys. Rev. D Part. Fields* **2007**, *75*, 025022. [CrossRef]
31. Almeida, C.A.S.; Casana, R.; Ferreira, M.M.; Gomes, A.R. Fermion localization and resonances on two-field thick branes. *Phys. Rev. D Part. Fields* **2009**, *79*, 125022. [CrossRef]
32. Liu, Y.-X.; Zhao, Z.-H.; Wei, S.-W.; Duan, Y.-S. Bulk matters on symmetric and asymmetric de sitter thick branes. *J. Cosmol. Astropart. Phys.* **2009**, *2009*, 003. [CrossRef]